Distributions of Chain Ends and Junction Points in Ordered Block Copolymers

A. M. Mayes, R. D. Johnson, and T. P. Russell*

Almaden Research Center, IBM Research Division, 650 Harry Road, San Jose, California 95120-6099

S. D. Smith

Procter and Gamble Company, Cincinnati, Ohio 45239-8707

S. K. Satija and C. F. Majkrzak

Reactor Radiation Division, National Institute of Standards and Technology, Gaithersburg, Maryland 20899

Received September 4, 1992; Revised Manuscript Received November 10, 1992

ABSTRACT: Chain configurations in ordered symmetric poly(styrene-*b*-methyl methacrylate) diblock copolymers were examined by neutron reflectivity. In a thin-film geometry the copolymers organize into lamellar microdomains oriented parallel to the substrate surface. The copolymers were synthesized with small fractions of deuterated segments at either the chain ends or centers. This selective labeling permitted characterization of the spatial distribution of chain ends and junction points normal to the plane of the film. From the reflectivity analysis, the junction points are found to be confined to the PS/PMMA interfacial regions. The chain ends, however, are well distributed through their respective domains, exhibiting only a weak maximum in concentration at the center of the domains.

Introduction

Over the past 2 decades a wealth of literature has appeared on the subject of A-*b*-B diblock copolymers and their equilibrium microdomain morphologies in the bulk.[1] At present, four ordered microdomain structures have been established experimentally as stable phases of pure copolymer melts in strong segregation,[2,3] and a fifth equilibrium morphology has been suggested for weakly ordered diblocks.[4,5] Until recently, transmission electron microscopy and small-angle X-ray scattering techniques served almost exclusively as tools for characterization of the various microdomain morphologies. These techniques are well suited for determining the structure and periodicity of the ordered phases as well as the average thicknesses of the copolymer microdomains. However, both methods are relatively insensitive for describing the interfacial region between A and B domains. Moreover, the spatial configuration of the copolymer blocks within the domains can only be inferred from the results, typically by comparing the observed dimensions of the microdomains with the Gaussian coil dimensions of the copolymer blocks. Along these lines, numerous studies have shown that copolymer blocks in strongly segregated domains are extended in the direction normal to the interface.

To gain more detailed information on chain configurations in ordered copolymer morphologies, several groups have performed small-angle neutron scattering on selectively deuterated copolymer systems.[6-8] Hadziioannou et al.[6] analyzed the lateral extension of polystyrene blocks in lamellar poly(styrene-*b*-isoprene) morphologies by adding dilute concentrations of diblocks with perdeuterated styrene segments to unlabeled copolymers of roughly equal molecular weight. The polystyrene chains were found to be contracted in the plane of the lamellae relative to their random coil dimensions. More recently, Matsushita et al.[8] performed SANS on ordered symmetric poly(styrene-*b*-2-vinylpyridine) copolymers in which portions (20–35%) of the styrene blocks were labeled with deuterium. In systems which were labeled adjacent to the copolymer junction points, the results were adequately modeled by assuming complete localization of the deuterated material near the PS/PVP interface. Similarly, for end-labeled copolymers the data were fit by assuming that the deuterated chain ends were perfectly centralized within the polystyrene domains. Although some localization of junction points and chain ends is certainly expected, the ability to describe the data using these coarse models of the concentration profiles suggests that SANS is somewhat insensitive to the true label distribution. Nevertheless, the results of Matsushita et al.[8] qualitatively indicate that the copolymer junction points and chain ends are to some degree localized within ordered lamellar domains. In the present study, neutron reflectivity is used to examine this question more quantitatively for symmetric poly(styrene-*b*-methyl methacrylate) copolymers in which a small fraction (5–10%) of either block has been deuterated at the chain end or adjacent to the PS/PMMA junction.

In previous studies, neutron reflectivity has demonstrated remarkable sensitivity to the scattering length density distribution normal to the surface in thin films of selectively labeled symmetric P(S-*b*-MMA) copolymers[9,10] and copolymer/homopolymer blends[11] on silicon substrates. Through a preferential interaction of the PMMA blocks with the substrate and the PS blocks with the surface, a near-perfect orientation of the lamellar domains is established parallel to the Si surface. For copolymers consisting of fully deuterated PS or PMMA blocks, neutron reflectivity has provided detailed information on the average domain sizes and interfacial widths as a function of copolymer molecular weight.[10] In the present study, selected portions of the PS or PMMA blocks are deuterated to reveal a quantitative picture of the spatial distribution of labeled segments within the ordered domains. In qualitative agreement with Matsushita et al.,[8] localization of center labels and end labels is observed. Quantitatively, however, the spatial distributions of the labels obtained here differ significantly from those determined from the SANS analysis of PS-*b*-PVP.

0024-9297/93/2226-1047$04.00/0

Experimental Section

Polished silicon substrates 10 cm in diameter and 0.5 cm thick with (100) crystal planes parallel to the surface were purchased from Semiconductor Processing Co. Substrates were submerged in Chromerge overnight, rinsed thoroughly with deionized water, and air-dried. Prior to use, substrates were immersed in sulfuric acid and Nochromix for 5 min, rinsed with deionized water, exposed to 2-propanol vapor for 5 min, and subsequently dried at 110 °C.

The copolymers were synthesized using standard anionic techniques. Cyclohexane (Phillips Petroleum) was stirred over sulfuric acid for 1 week and then distilled from calcium hydride. Tetrahydrofuran (Fisher) was distilled from sodium benzophenone ketal. Dibutylmagnesium and *sec*-butyllithium were used as received from Lithium Corp. of America. Triethylaluminum (Aldrich) was used as received. Methyl methacrylate (Aldrich) and methyl methacrylate-d_8 (Cambridge Isotope Labs) were purified by treatment with triethylaluminum and were subsequently distilled under vacuum.[12] Styrene (Aldrich) and perdeuterated styrene (Cambridge Isotope Labs) were passed through an alumina column to remove inhibitors, then titrated with dibutylmagnesium to eliminate impurities, and finally passed through an activated alumina column to remove magnesium salts. 1,1-Diphenylethylene (Kodak) was purified by the reaction of impurities with *sec*-butyllithium followed by vacuum distillation.

The block copolymer synthesis was carried out in round-bottom flasks, equipped with septa, using magnetic stirring under a nitrogen atmosphere. Typically 20% solutions of styrene in cyclohexane were prepared along with 1% by volume tetrahydrofuran. The styrene blocks were initiated with *sec*-butyllithium and allowed to grow for 15 min, at which time further quantities of purified perdeuterated styrene or styrene monomers were added to grow the desired sequences of labeled segments. The styryllithium chains were capped with 1,1-diphenylethylene to produce a more sterically hindered carbanion. This carbanion has been shown to initiate methyl methacrylate polymerization without the undesired addition to the carbonyl that occurs with styryllithium.[13] The reactions were diluted with purified tetrahydrofuran to minimally 75 vol % THF and were then cooled to −78 °C. Purified methyl methacrylate or deuterium-labeled MMA was then added dropwise to the polymerization. It is necessary to add the monomer slowly to maintain the reaction temperature below −60 °C to avoid side reactions. The MMA polymerization is extremely rapid, and the polymerization of MMA monomer under these conditions is essentially complete within 60 s. Five minutes was allowed for complete monomer consumption, and the buildup of MMA-*b*-d-MMA sequences was accomplished by the sequential addition as desired. The polymer solutions were precipitated into a 10-fold excess of methanol and vacuum-dried. Soxhlet extraction with cyclohexane was found to be efficient at removing any free polystyrene homopolymer which resulted from killing of the first block.

Molecular weights and molecular weight distributions were determined by size exclusion chromatography with Ultrastyragel columns of 10^3-, 10^4-, and 10^5-Å porosities in tetrahydrofuran. The volume fraction of styrene segments in the copolymer was determined using ^{1}H NMR after correction for the number of labeled segments in the chain. To determine the composition of the hydrogenous components (styrene and methyl methacrylate segments), ^{2}H NMR spectra were recorded on an IBM Instruments AF300, operating in an unlocked mode at a ^{2}H frequency of 46.3 MHz. Spectra were collected using a 15-μs pulse width, corresponding to a 90° excitation angle, with typically 500 scans digitized into 8K data points. A 15-s relaxation delay between scans, more than 5 times the longest T_1 in the sample, ensured all resonances were fully relaxed before each acquisition. Both the polymer solution in the NMR tube and the calibrant solution in the coaxial insert tube were vertically positioned so as to be within the ^{2}H rf coil during the NMR experiments, ensuring equivalent rf excitation and detection for both solutions. Anthracene-d_{10} (97.9% atom ^{2}H) was purchased from MSD Isotopes; the NMR shift reagent Dy(fod)$_3$ was obtained from Aldrich Chemical Co.

Thin films of the copolymers were prepared by spin casting from toluene solutions of approximately 3 wt/vol %. Samples were cast onto silicon substrates at 2000 rpm to give film thicknesses between 1300 and 1600 Å. Film thicknesses were measured by ellipsometry prior to annealing. Specimens were annealed under vacuum at 160 °C for 10 days to achieve ordering.

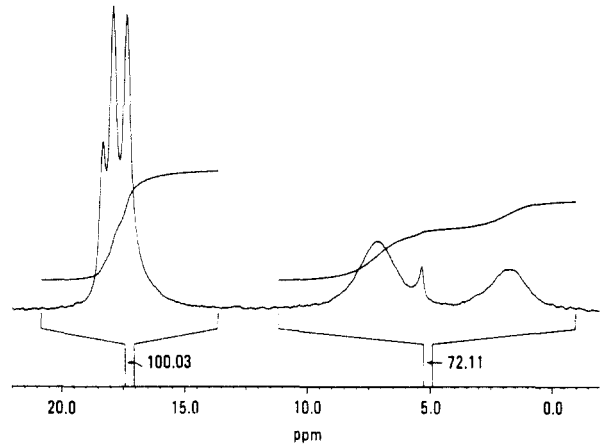

Figure 1. ^{2}H NMR spectrum of 50 mg of P(d-S-*b*-S-*b*-MMA) in CH_2Cl_2 and a tube insert containing 3.5 mg of anthracene-d_{10} and 8 mg of Dy(fod)$_3$ dissolved in $CHCl_3$. Integration of the anthracene vs polymer resonances yields 1.88 mg of d-PS present in the solution; hence 2.4% of the monomers are deuterated.

Neutron reflectivity measurements were performed on the BT-7 instrument at the National Institute of Standards and Technology. The experimental setup and sample alignment procedure have been described in detail elsewhere.[9-11] A graphite monochromator was used to deliver neutrons of wavelength λ = 2.37 Å and $\Delta\lambda/\lambda \approx 0.01$. Reflectivity curves were generated by rotating the sample θ and the detector 2θ degrees with reference to the incident beam. Data points were taken in steps of 0.01° in θ out to 1.5° or 0.07 Å^{-1} in neutron momentum, $k_{z,0} = (2\pi/\lambda) \sin\theta$. Background intensities were obtained by offsetting 2θ by +0.25°. Background was taken in 0.05° steps in θ and extrapolated linearly between points. After background subtraction the net intensity was divided by the main beam intensity to produce the reflectivity profiles.

Deuterium Content

A quantitative determination of the deuterium label content of the block copolymer was accomplished by solution ^{2}H NMR, which is capable of furnishing accurate relative mole fractions of mixtures. When saturation effects are avoided, the area of a peak in the spectrum faithfully reports the relative amount of nuclei corresponding to that specific resonance.[14] Absolute amounts of nuclei in a sample can be determined by measuring the peak area of a known amount of added material which serves as a calibrant for the other resonances of interest. However, this approach is problematical for ^{2}H NMR of labeled polymers, since the ^{2}H NMR line widths for macromolecules are typically large enough to contribute to the whole diamagnetic region of the ^{2}H NMR spectrum, thus preventing resolution of polymer peaks from those of the added calibrant molecules.

This problem was avoided by physically separating the polymer solution from the added calibrant by placing a solution of the latter in a glass tube inserted into an NMR tube containing the polymer solution. An NMR shift reagent, Dy(fod)$_3$, was then added to the calibrant solution to shift the calibrant NMR resonances downfield, well away from the polymer resonances.[15] The resultant NMR spectrum of this system yielded two sets of resonances, those arising from the polymer and those arising from the shifted calibrant molecules. A typical result is shown in Figure 1, where the insert tube contained 3.5 mg of anthracene-d_{10} and Dy(fod)$_3$ and the solution in the NMR tube contained 50 mg of the partially deuterated copol-

Table I
Characteristics of Copolymers

copolymer	M_w	M_w/M_n	$f^a_{PS,NMR}$	$f^b_{PS,NR}$	deuterium content: $^2H^c$	$^2H_3CCl^d$	A^e	f^f_{NMR}	f^g_{NR}
P(d-S-*b*-S-*b*-MMA)	180K	1.21	0.46	0.48	3.1	2.5	2.4	2.3	2.2
P(S-*b*-d-S-*b*-MMA)	100K	1.13	0.42	0.43	2.6	2.7	2.7	2.7	2.6
P(S-*b*-MMA-*b*-d-MMA)	70K	1.13	0.48	0.47	7.0	6.2	5.6	5.0	5.2

[a] PS volume fractions from ^1H NMR corrected for deuterium content. [b] PS volume fractions from fits to the neutron reflectivity profiles. [c] ^2H NMR percentage of labeled monomer with respect to the total number of monomers obtained by using deuterated chloroform. [d] ^2H NMR number percents using deuterated chloroform and Dy(fod)$_3$. [e] ^2H NMR number percents using deuterated anthracene and Dy(fod)$_3$. [f] Volume fraction of labeled material calculated from anthracene ^2H NMR results. [g] Volume fraction of labeled material from fits to the neutron reflectivity profiles.

Table II
Scattering Length Densities of Components

material	density (g/cm^3)	(b/V) ($\times 10^{-6}$ Å^{-2})
PMMA	1.15	1.0
d-PMMA	1.24	6.8
PS	1.06	1.43
d-PS	1.14	6.1
Si	2.32	2.08
SiO_2	2.20	3.48

ymer. The anthracene resonances were shifted downfield to 19 ppm, while the polymer resonances appeared in the region 8 to 0 ppm. The anthracene and polymer resonances were then easily integrated, with the anthracene integral corresponding to the ^2H present in 3.5 mg of labeled anthracene. The ratio of integrals yielded the amount of ^2H present in the polymer solution. The amount of ^2H-labeled polystyrene was then obtained, and hence the fraction in the copolymer sample. Results for the four copolymer samples are presented in Table I. Additional composition results for these polymers were calculated by using C^2HCl_3 in place of anthracene-d_{10} and by adding directly a known amount of deuterated solvent to the polymer solution and then obtaining the polymer/solvent ratio by deconvolution of the resultant NMR spectrum. Table I shows all three methods to be in good agreement.

Model Reflectivity Profiles

In specular reflectivity, radiation incident on a surface at a glancing angle θ is detected at a corresponding angle θ from the surface after undergoing reflection, thereby recording the momentum transfer perpendicular to the surface. The coefficient of reflectivity at an interface between two media depends upon the neutron refractive index of each medium, which is given by

$$\eta_j = \left[1 - \frac{\lambda^2}{2\pi}(b/V)_j\right]^2$$

where $(b/V)_j$ is the scattering length density of the medium j. Scattering length density values for materials relevant to this study are provided in Table II. If the scattering length density varies through the thickness of a film, the reflectivity can be approximated by dividing the film into j layers of an arbitrary thickness d_j and scattering length density $(b/V)_j$. For each layer the reflection coefficient can be determined exactly. By use of recursion formulas based on Fresnel optics the reflectivity R can be calculated as a function of incident neutron momentum, $k_{z,0}$, to compare with the experimentally obtained profile.[16]

For cases where either the PS or PMMA blocks are fully deuterated, the reflectivity for ordered P(S-*b*-MMA) copolymer films is well described by model composition profiles which consist of alternating domains of PS and PMMA with hyperbolic tangent concentration profiles across the interfaces. In the present study, however, the copolymers contain only small fractions of deuterated PS or PMMA segments. Thus, the systems are effectively composed of three components, and the labeled segment distribution must be deconvoluted from the distribution of PS and PMMA using the known volume fractions for the three components. For chain-end labeled systems, label distributions were modeled by dividing the corresponding copolymer domains into incremental layers of ~7 Å in thickness. The (b/V) value for each layer was calculated assuming a normal distribution of the labeled material about the center of the domain, decaying to some base value at the domain boundaries. In the two extremes for this model, the end labels can be either entirely confined to the domain center, represented by a sharp Gaussian distribution, or uniformly distributed through the domain, such that the scattering length density across the domain is uniform. For center-labeled systems a similar model was used with the hydrogenated rather than deuterated material centrally distributed in the domains. For both cases, hyperbolic tangent interfacial profiles were used to describe the interface between PS and PMMA domains. Model parameters, including the full-width half-maximum and base value of the scattering length density in each domain, the domain widths, and the interfacial thicknesses, were determined using an iterative fitting procedure to minimize the difference between the calculated reflectivity curves and the experimental data. The interfacial thicknesses were restricted within limits consistent with the average values for copolymers of comparable molecular weight having fully deuterated blocks of PS or PMMA.[11] For each system, the relative fractions of PS, PMMA, and labeled PS or PMMA in the calculated volume fraction profiles are consistent with the composition characteristics of the copolymers as shown in Table I. In all cases, a 10–20-Å-thick oxide layer on the silicon surface was incorporated into the model scattering length density profiles.

Results

Figure 2 shows the reflectivity profile for an end-labeled P(S-*b*-MMA-*b*-d-MMA) block copolymer containing 5.0 ± 0.5 vol % labeled material. The open circles represent the experimental data, while the solid line indicates the model reflectivity generated by the scattering length density profile inset in the figure. (Error bars in the experimental data have been omitted for purposes of clarity.) The decrease in the reflectivity for angles below the critical angle is a consequence of the finite sample size. The Bragg reflections observed in the profile indicate a high degree of ordering parallel to the substrate. The low peak intensities, however, reveal significant intermixing between the unlabeled and labeled PMMA segments. The model scattering length density profile indicates 4.5 copolymer layers are present in the film. The depression in the scattering length density in the first copolymer layer, i.e., adjacent to the air, is attributed to the presence of holes on the film surface which result from

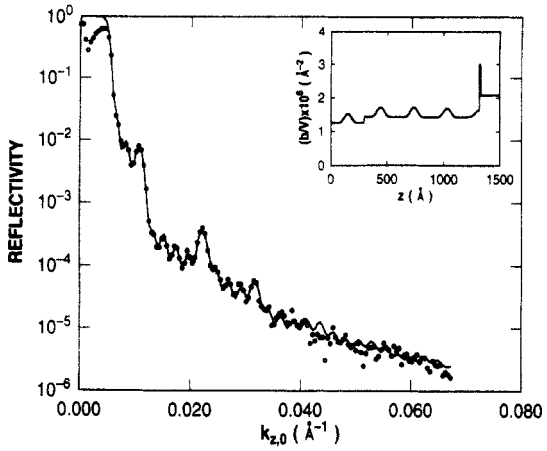

Figure 2. Neutron reflectivity as a function of the neutron momentum for a P(S-*b*-MMA) symmetric, diblock copolymer where a fraction of the MMA end of the copolymer was labeled with deuterium. The solid line was the best fit to the data (open circles) using the scattering length density profile shown in the inset.

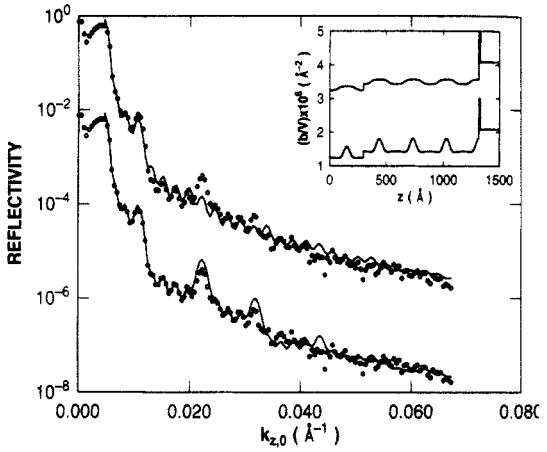

Figure 3. Same data as in Figure 2 but where the calculated profiles are for the case where the chain ends were assumed to be more centralized to the lamellar domains (lower curve) and for a uniform distribution of chain ends in the domain (upper curve). The profiles have been offset for clarity. The model scattering length density profiles and shown in the inset.

finite film thickness constraints. Earlier studies found that P(S-*b*-MMA) copolymer films on Si substrates order such that the equilibrium thickness of the system is quantized to $(n + 1/2)L$, where n is an integer and L is the period of the diblock copolymer.[17,18] If the thickness of the film when originally cast does not closely correspond to $n + 1/2$ periods, the system satisfies this constraint by the formation of islands or holes on the film surface; the height of each satisfies the $(n + 1/2)L$ condition. This phenomenon has been extensively studied by Coulon and co-workers[19,20] using optical and atomic force microscopy.

When a hole concentration of ~15% is taken into account at the surface, the label distributions within the PMMA domains are quite comparable throughout the thickness of the film. The model (b/V) profile indicates some centralization of the labeled ends within the PMMA domains. The sensitivity of the reflectivity profiles to the label distribution is demonstrated in Figure 3, which shows calculated reflectivity curves assuming a more centralized chain-end distribution in the PMMA domains (lower curve) and a uniform chain-end distribution (upper curve). Both models give notably worse fits than that shown in Figure 2, although the model (b/V) profiles differ only slightly.

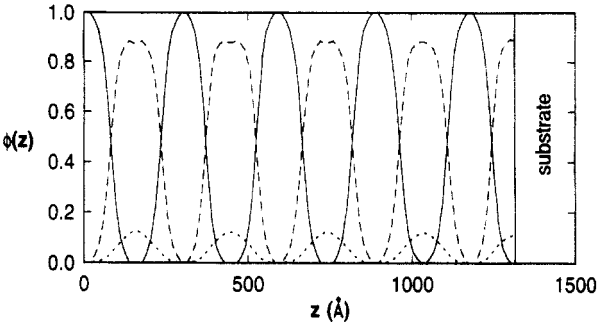

Figure 4. Volume fraction of the styrene, methyl methacrylate, and labeled methyl methacrylate chain ends as a function of depth normal to the surface. These volume fractions were derived from the scattering length density profile shown in the inset of Figure 2.

To convert the scattering length density profile in Figure 2 to a volume fraction profile, the interface between PS and PMMA domains must be assumed. Since the reflectivity for this system is quite insensitive to the width and position of the interfacial regions, the interfacial widths were fixed between 45 and 55 Å as determined in previous studies,[9,10] while their positions were set by the ratio of PS to PMMA + d-PMMA in the copolymer. Figure 4 shows the volume fraction profile consistent with the scattering length density profile inset in Figure 2. The PS and PMMA block distributions are represented by the solid and dashed curves, respectively. The labeled PMMA chain ends, indicated by the dotted curves, are well distributed through the PMMA domains, with a small concentration maximum occurring in the domain centers. The PMMA chain ends appear to penetrate well into the interfacial regions. At the interface between the film and the substrate, the distribution of labeled material in the PMMA half-layer is quite similar to that in the internal PMMA domains. This implies that no significant deuteration effect is observed at this film boundary; i.e., there is no preferential segregation of the deuterated chain ends to the substrate. Moreover, the configurations of the PMMA chains within this layer do not seem to differ significantly from the chain configurations in interior of the film, irrespective of the hard-wall constraint at the substrate. It should be noted that the scattering length density of SiO_2 is between that of the Si substrate and the PMMA. This leads to some ambiguity in defining precisely the chain-end distribution at the substrate. Consequently, a more quantitative statement cannot be made.

With reduced labeling content, a quantitative interpretation of the reflectivity profile becomes more difficult. Figure 5 shows the reflectivity curve obtained for an end-labeled P(d-S-*b*-S-*b*-MMA) copolymer with 2.3 ± 0.5 vol % labeling. For this system the higher order Bragg reflections are hard to distinguish from thickness fringes, and the primary reflection is also extremely weak. Although the system is well ordered, as evidenced by hole formation observed on the film surface by optical microscopy, the contrast between PS and PMMA domains is extremely low. The lack of features in the reflectivity profile is an immediate indication that, as seen for the previous system, the labeled chain ends are well distributed throughout the PS domains rather than being concentrated in the domain centers. These results contrast those of Matsushita et al.,[8] which suggest that complete segregation of labeled chain ends to the domain centers occurs. The volume fraction profile which corresponds to the scattering length density model in the inset of Figure 5 is shown in Figure 6. Similar to what is seen in Figure 4, the distribution of PS chain ends is slightly centralized within

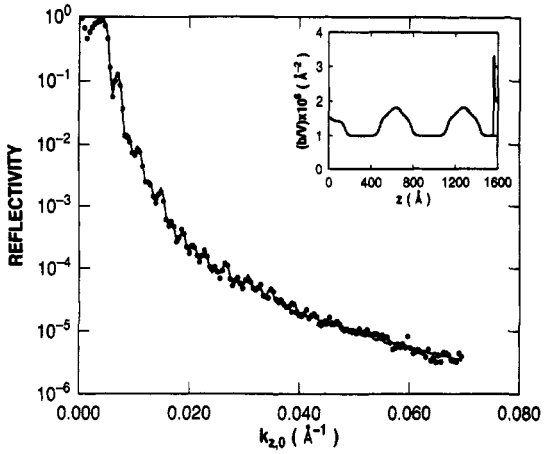

Figure 5. Neutron reflectivity as a function of the neutron momentum for a P(d-S-*b*-S-*b*-MMA) copolymer where a fraction of the styrene units at the chain ends was labeled with deuterium. The solid line was the best fit to the data using the scattering length density profile shown in the inset.

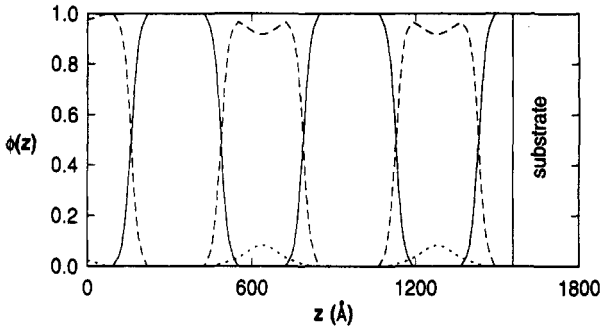

Figure 6. Volume fraction of the labeled styrene, styrene, and methyl methacrylate segments as a function of depth in the specimen. These were derived from the scattering length density profile shown in the inset of Figure 5.

the PS domains in the film's interior. However, less penetration of the chain ends into the interfacial regions is indicated, presumably because the block molecular weight is substantially higher (180K versus 70K), while the fraction of labeled material is much lower. The presence of holes (or islands) on the surface of the copolymer leads to a reduction in the scattering length density of the layer adjacent to the air surface in the model calculations.[11] Consequently, within the PS half-layer at the film surface, the label distribution could not be characterized adequately.

For the two systems studied above, placement of the labeled copolymer chain ends within the corresponding domains is apparently dominated by entropic considerations. Chain ends are found to sample the whole width of the domains, rather than just the domain centers, as one might anticipate for highly stretched chains. By comparison, placement of the copolymer junction points should be controlled by strong energetic restrictions which favor their confinement to the interfacial regions. In Figure 7, the reflectivity profile for a center-labeled P(S-*b*-d-S-*b*-MMA) copolymer containing 2.7 ± 0.5 vol % labeled material is shown. In contrast to the data in Figure 5, strong reflections are evident in the reflectivity profile for this system, indicating significant localization of the deuterated chain centers. The model scattering length density profile inset in the figure clearly shows maxima in the label distribution near the PS/PMMA interfaces. The volume fraction profile consistent with this model is given in Figure 8. The majority of the d-PS (dashed curve) is localized within the interfacial regions (the regions of

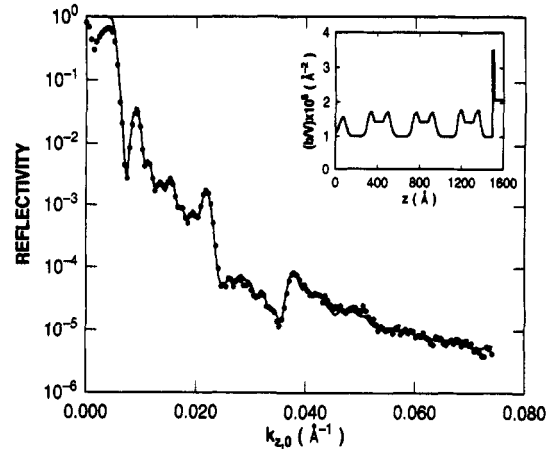

Figure 7. Neutron reflectivity as a function of the neutron momentum for a P(S-*b*-MMA) symmetric, diblock copolymer where the styrene segments adjacent to the junction points were labeled with deuterium. The scattering length density profile shown in the inset yielded the best fit to the data indicated by the solid line.

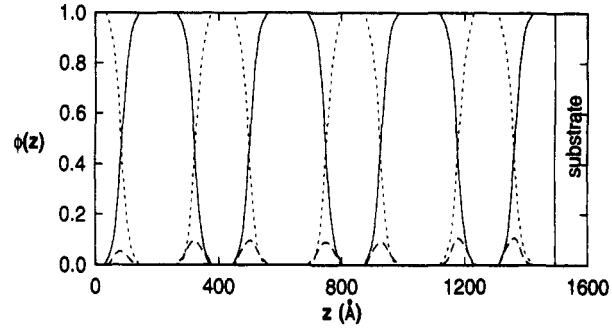

Figure 8. Volume fraction of the styrene, labeled styrene, and methyl methacrylate segments as a function of distance from the surface derived from the scattering length density profile shown in the inset of Figure 7.

overlap of the solid and dotted curves). An asymmetric distribution of the labeled material (dashed curve) is indicated. Considering that the label distribution does not represent a single junction point but a finite length chain (~25 segments) of d-PS, this asymmetry is not surprising.

The observed localization of the chain centers to the interfacial regions agrees qualitatively with the conclusions of Matsushita et al.[8] However, we again find discrepancies in the quantitative results of the two studies. In the previous study, the data were fit assuming total segregation of the center labels at the interface with a scattering length density characteristic of the pure deuterated material. In the present study, the d-PS segments adjacent to the junction points are clearly intermixed with PMMA and unlabeled PS units.

Conclusions

In this study neutron reflectivity has been used to gain very detailed descriptions of the segment distributions in ordered symmetric copolymers not obtainable by other techniques. For end-labeled copolymers, the labeled material is shown to be well distributed within the corresponding domains, with small maxima in the label distributions occurring at the domain centers. With possible implications to ordered symmetric A–B–A triblocks, this result suggests that looped center-block configurations are possible in addition to B configurations which bridge the two adjacent A domains. For center-labeled polymers, the label distribution is observed to be

more localized and asymmetric. In both cases, the results from neutron reflectivity, although qualitatively confirming the results of Matsushita et al.,[8] are in quantitative disagreement. The discrepancies between the two studies may arise from several factors. First, the previous study analyzed systems with a significantly higher label content than the systems discussed here. Second, the PS-*b*-PVP is more strongly segregated, with sharper interfaces and more highly stretched copolymer blocks than the PS-*b*-PMMA systems studied here. In principle, this would increase the localization of both the chain ends and chain centers. Having mentioned this, it is most likely that reflectivity is simply more sensitive to the fine details of the distribution that can be obtained by other scattering techniques. Reflectivity arises from gradients in the refractive index whereas scattering techniques measure correlations in the refractive index. Thus, the scattering measurements incorporate interferences not related to the problem of interest which must be removed from the data prior to analysis. Reflectivity measurements currently in progress[21] on thin films of PS-*b*-PVP symmetric, diblock copolymers should shed new light on the effect of χ in defining the spatial distribution of the copolymer chains in the multilayered, lamellar morphology. These studies will be directly comparable to the small-angle neutron scattering studies of Matsushita et al.[8] In addition, a quantitative comparison between the sensitivity of neutron reflectivity and small-angle scattering can be made which should aid in future comparison of results from both techniques.

Acknowledgment. The authors are indebted to G. R. May of the IBM Almaden Research Center for assistance with the NMR measurements. This work was supported, in part, by the Department of Energy, Office of Basic Energy Sciences, under Contract DE-FG03-88ER45375.

References and Notes

(1) *Developments in Block Copolymers—I*; Goodman, I., Ed.; Applied Science: New York, 1985.
(2) Hasegawa, H.; Tanaka, H.; Yamasaki, K.; Hashimoto, T. *Macromolecules* **1987**, *20*, 1651.
(3) Thomas, E. L.; Anderson, D. M.; Henkee, C. S.; Hoffman, D. *Nature* **1988**, *334*, 598.
(4) Olvera de la Cruz, M.; Mayes, A. M.; Swift, B. W. *Macromolecules* **1992**, *25*, 944.
(5) Almdahl, K.; Koppi, K. A.; Bates, F. S.; Mortensen, K. *Macromolecules* **1992**, *25*, 1743.
(6) Hadziioannou, G.; Picot, C.; Skoulious, A.; Ionescu, M.; Mathis, A.; Gallot, Y.; Lingelser, J. *Macromolecules* **1982**, *15*, 263.
(7) Hasegawa, H.; Hashimoto, T.; Kawai, H.; Lodge, T. P.; Amis, E. J.; Glinka, C. J.; Han, C. C. *Macromolecules* **1985**, *18*, 67.
(8) Matsushita, Y.; Mori, K.; Mogi, Y.; Saguchi, R.; Noda, I.; Nagasawa, M.; Chang, T.; Glinka, C. J.; Han, C. C. *Macromolecules* **1990**, *23*, 4317.
(9) Anastasiadis, S. H.; Russell, T. P.; Satija, S. K.; Majkrzak, C. F. *Phys. Rev. Lett.* **1989**, *62*, 1852.
(10) Anastasiadis, S. H.; Russell, T. P.; Satija, S. K.; Majkrzak, C. F. *J. Chem. Phys.* **1990**, *92*, 5677.
(11) Mayes, A. M.; Russell, T. P.; Satija, S. K.; Majkrzak, C. F. *Macromolecules* **1992**, *25*, 6523.
(12) Allen, R. D.; Long, J. E.; McGrath, J. E. *Polym. Bull.* **1986**, *15*, 127.
(13) Freyss, D.; Rempp, P.; Benoit, H. *J. Polym. Sci., Polym. Lett. Ed.* **1964**, *2*, 217.
(14) Farrar, T. C. *Pulsed NMR Spectroscopy*; Farragut Press: Madison, WI, 1989.
(15) Horrocks, W. de W., Jr. In *NMR of Paramagnetic Molecules*; La Mar, G. N., Horrocks, W. de W., Jr.; Holm, R. H., Eds.; Academic Press: New York, 1973; Chapter 12.
(16) Russell, T. P. *Mater. Sci. Rep.* **1990**, *5*, 171.
(17) Coulon, G.; Russell, T. P.; Deline, V. R.; Green, P. F. *Macromolecules* **1989**, *22*, 2581.
(18) Russell, T. P.; Coulon, G.; Deline, V. R.; Miller, D. C. *Macromolecules* **1991**, *22*, 4600.
(19) Coulon, G.; Collin, B.; Ausserre, D.; Chatenay, D.; Russell, T. P. *J. Phys. Fr.* **1990**, *51*, 2801.
(20) Collin, B.; Chatenay, D.; Coulon, G.; Ausserre, D.; Gallot, Y. *Macromolecules* **1992**, *25*, 1621.
(21) Karim, A., private communication.